Proceedings of the 18th International Conference on Nuclear Engineering
ICONE18
May 17-21, 2010, Xi'an, China

ICONE18-29198

3D SIMULATION OF MOLTEN METAL FREEZING BEHAVIOUR USING FINITE VOLUME PARTICLE METHOD

Rida SN Mahmudah, Masahiro Kumabe, Takahito Suzuki, LianCheng Guo, Koji Morita, Kenji Fukuda
Kyushu University
744 Motooka Nishi-ku, Fukuoka 819-0395, Japan

ABSTRACT

Understanding the freezing behavior of molten metal in flow channels is of importance for severe accident analysis of liquid metal reactors. In order to simulate its fundamental behavior, a 3D fluid dynamics code was developed using Finite Volume Particle (FVP) method, which is one of the moving particle methods. This method, which is fully Lagrangian particle method, assumes that each moving particle occupies certain volume. The governing equations that determine the phase change process are solved by discretizing its gradient and Laplacian terms with the moving particles. The motions of each particle and heat transfer between particles are calculated through interaction with its neighboring particles. A series of experiments for fundamental freezing behavior of molten metal during penetration on to a metal structure was also performed to provide data for the validation of the developed code. The comparison between simulation and experimental results indicates that the present 3D code using the FVP method can successfully reproduce the observed freezing process such as molten metal temperature profile, frozen molten metal shape and its penetration length on the metal structure.

1. INTRODUCTION

The freezing behavior of molten metal in flow channel is one of the major concerns for safety analysis of the liquid metal cooled reactor (LMR). In hypothetical core disruptive accidents (CDAs) of LMR, interaction of molten fuel and structure can occur when serious transient over power and transient under cooling accident take place [1]. The first is power increase beyond control and the latter is slow flowing of coolant. Both of those transient behaviors will lead to increase of core temperature which will lead to other accident sequences, such as cladding melting, disruption of fuel, and fuel release into coolant.

It is anticipated that during CDA of LMR molten cladding and disrupted fuel flow through subassembly channels. Due to interactions of the molten metal with coolant and structure, heat is transferred from the molten metal to the coolant and structure. When the internal energy loss of molten metal due to the heat transfer is exceeded the latent heat of molten metal, the molten metal become freeze and penetrate the structure. This penetration of molten metal onto the structure will cause blockages in the channel. Although the occurrence of CDA is extremely unrealistic due to the denying actuations of all multiple safety systems, it is still emphasized from the viewpoint of safety design and evaluation.

Many studies of liquid metals freezing in structure have been conducted for safety analysis of reactor severe accidents [2-6]. Rahman, et al [7], have performed experiment of molten metal freezing on various coolant systems and to investigate this freezing molten metal behavior on flow channel. The numerical simulation of the experimental results was performed by the reactor safety analysis code SIMMER-III using a mixed freezing model involving both bulk freezing and crust formation on the structure [8]. This present study has similar objective, but unlike the previous work, the numerical calculation in this study was performed using a moving particle method.

It would be difficult for conventional mesh methods to directly simulate such complicated flows with freezing phase change since it is necessary to capture liquid-solid interphase every time. Several moving particle methods, such as smoothed particle hydrodynamics (SPH) method [9], moving particle semi-implicit (MPS) method [10], and finite volume particle (FVP) method [11] etc, which are a fully lagrangian methods, have been developed in the recent years. Unlike mesh methods, there is no need for interphase construction in the moving particle methods, because each moving particle represents each phase with specific physical

properties. Therefore, the simulation of freezing behavior of molten metal can performed straightforwardly.

In this study, a 3D fluid dynamics code using the FVP method was developed. It simulates molten wood's metal flows and freezes on L-shaped conduction wall. Penetration length of the molten wood's metal was calculated to validate the heat transfer and phase change model incorporation with FVP. To provide data for validating the developed code, a series of experiments for fundamental freezing behavior was performed. A comparison between experiments and simulations demonstrated that coupled calculation of multi-phase flow fluid dynamics and phase change calculation using FVP method is effective and representing reasonably good result.

2. NUMERICAL METHOD

2.1. Governing Equations

The governing equations for the incompressible fluids are the Navier-Stokes equation, the equation of continuity and energy conservation equation:

$$\frac{D\vec{u}}{Dt} = \frac{1}{\rho}\nabla P + \frac{1}{\rho}\nabla\cdot(\mu\nabla\vec{u}) + \vec{g} + \vec{f} \quad (1)$$

$$\nabla\cdot\vec{u} = 0 \quad (2)$$

$$\frac{D(\rho h)}{Dt} = \nabla\cdot(k\nabla T) + Q \quad (3)$$

These governing equations are solved by discretizing its gradient and laplacian terms with the FVP method. These discretized governing equations are then solved by Combined and Unified Procedure (CUP) algorithm [12]. A comprehensive and complete explanation of this algorithm can be found on the reference [13].

2.2. FVP method

In the FVP method, which adopts the same concept as the conventional finite volume method, each particle is assumed to occupy a certain volume. The control volume of one moving particle is a sphere in 3D simulations:

$$S = 4\pi R^2, V = \frac{4}{3}\pi R^3 = (\Delta l)^2 \quad (4)$$

According to Gauss's law, the gradient and Laplacian operators are expressed by

$$\nabla\phi = \lim_{R\to 0}\frac{1}{V}\oint_V \nabla\phi dV = \lim_{R\to 0}\frac{1}{V}\oint_S \phi\vec{n}dS \quad (5)$$

$$\nabla^2\phi = \lim_{R\to 0}\frac{1}{V}\oint_V \nabla^2\phi dV = \lim_{R\to 0}\frac{1}{V}\oint_V \nabla\phi\cdot\vec{n}dS \quad (6)$$

As a result, in the FVP method the gradient and Laplacian terms can be approximated as

$$\langle\nabla\phi\rangle_i = \langle\frac{1}{V}\oint_S \phi\vec{n}dS\rangle_i = \frac{1}{V}\sum_{j\neq i}\phi_s\cdot\vec{n}_{ij}\cdot\Delta S_{ij} \quad (7)$$

$$\langle\nabla^2\phi\rangle_i = \langle\frac{1}{V}\oint_S \nabla\phi\cdot\vec{n}dS\rangle_i = \frac{1}{V}\sum_{j\neq i}\left(\frac{\phi_j-\phi_i}{|\vec{r}_{ij}|}\right)\cdot\Delta S_{ij} \quad (8)$$

Schematic diagram of neighboring particles around particle *i* within the cut-off radius is shown in Figure 1.

The interaction surface of particle j with particle *i*, ΔS_{ij}, can be calculated by

$$\Delta S_{ij} = \frac{\omega_{ij}}{n^0}S \quad (9)$$

The initial number density, n^0, is calculated as

$$n^0 = \sum_{j\neq i}\omega_{ij} \quad (10)$$

The value of n^0 is set to the number density of a particle which is not near or on boundaries. The unit vector of the distance between two particles, $\vec{n}_{ij}$, is expressed by

$$\vec{n}_{ij} = \frac{\vec{r}_{ij}}{|\vec{r}_{ij}|} \quad (11)$$

The kernel function ω_{ij} is defined as

$$\omega_{ij} = \sin^{-1}\left(\frac{R}{|\vec{r}_{ij}|}\right) - \sin^{-1}\left(\frac{R}{r_e}\right) \quad (12)$$

where r_e is the cut-off radius and is usually chosen as $2.1\Delta l$ for the 3D systems. If the distance between two particles is larger than the cut-off radius, the kernel function is set as zero. Using Eqs. (9), (10) and (11), Eqs. (7) and (8) can be rearranged as

$$\langle\nabla\phi\rangle_i = \frac{S}{Vn^0}\sum_{j\neq i}\left(\phi_i + \frac{\phi_j-\phi_i}{|\vec{r}_{ij}|}R\right)\omega_{ij}\,\vec{n}_{ij} \quad (13)$$

$$\langle\nabla^2\phi\rangle_i = \frac{S}{Vn^0}\sum_{j\neq i}\frac{\phi_j-\phi_i}{|\vec{r}_{ij}|}\omega_{ij} \quad (14)$$

With this gradient and Laplacian models, the governing equations can be easily discretized.

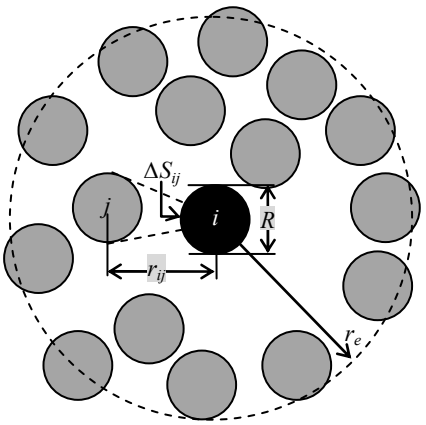

Fig. 1 Neighboring particles around particle i within the cut-off radius

2. 2. Phase Change Model

The governing equation that determines the phase change process, Eqs. (3), can be expressed as [14]

$$\rho\frac{Dh}{Dt} = k\nabla^2 T + Q \quad (15)$$

The laplacian term in the above equation is approximated by Eqs (14). Thermal conductivity coefficient between particle *i* and particle *j*, k_{ij}, is defined as

$$k_{ij} = \begin{cases} k_j & \text{if particle } i \text{ is a mixture} \\ k_i & \text{if particle } j \text{ is a mixture} \\ \dfrac{2k_i k_j}{k_i + k_j} & \text{otherwise} \end{cases} \quad (16)$$

Phase change process in this study is treated as equilibrium heat transfer at phases interface. The phase change is determined when the solid particle's temperatures exceed the melting temperature or when the liquid particle's temperatures drop below freezing temperature. The interface temperatures of wall conduction-fluid particles and solid-liquid particles where phase change occurs are the melting/freezing temperature of particle

$$T_i = T_{m/f} \qquad 0<\alpha_i < 1 \qquad (17)$$

The phase change rate to the solid or liquid phase is expressed as the linear change during the freezing process, while the unchanging phase can be recognized as rigid solid or fully liquid.

$$\alpha_i = 0 \qquad h_i < h_s$$
$$\alpha_i = \frac{(h_i - h_s)}{(h_l - h_s)} \qquad h_s < h_i < h_l$$
$$\alpha_i = 1 \qquad h_l < h_i$$

2. 3. Viscosity Model

In order to correctly simulate the penetration of molten metal into a cold channel structure, it is important to simulate the effective increase in the fluid viscosity of the molten metal. Choosing an appropriate viscosity model also help us to deal with velocity suppression when liquid particle become solid. This is because the Navier-Stokes equation is being solved for the whole domain, thus a special treatment is needed to make frozen particle penetrate onto the wall. The simplest and most straightforward approach is to assign the particle velocity to zero when its temperature is below the freezing or solid temperature [15]. Another method is to set the viscosity as a function of fluid's temperature [15],[16]. If liquid turns into solid, the viscosity increases to a large value which suppresses the velocity. There are many viscosity-temperature equations to be chosen from a lot of literature. The present study use an empirical law to approximate viscosity changes, which has been used to study rheological phenomena as [17]

$$\mu_{app} = \max\left(\mu_{\max}, \mu_{liq}\exp\left[-A\left(h_i - h_l / C_p\right)\right]\right) \quad (18)$$

where μ_{app} is the dynamic viscosity coefficient of particle, which is used in Eqs. (1). To maintain the numerical stability, the upper limit value $\mu_{\max}$ is defined as [18]

$$\mu_{\max} = \mu_{liq}\exp\left[-A\left(h_{i,\alpha=0.35} - h_l / C_p\right)\right] \quad (19)$$

In this study, A is set as 0.14 compared to experiment results.

3. EXPERIMENTAL SET UP

Figure 2 shows schematic diagram of experimental apparatus. The facility consists of a melt tank section and a flow channel section. The former is used to preserve and pour molten wood's metal and the latter is used to observe the penetration and freezing behavior of molten wood's metal.

The melt tank section consists of wood's metal pot and plug. The wood's metal pot is made of Teflon. The pot's neck has geometry 4 cm in length and 0.88 cm and 0.6 cm in diameter of upper and bottom neck, respectively. The plug, also made of Teflon, has cylinder shape with 20 cm in length and 1.4 cm in diameter, except at the edge of plug which contacts with the pot's neck. This plug edge has the same diameter as the upper pot's neck, which will prevent the leakages of molten wood's metal. The pouring of molten wood's metal to the conduction wall is made by pulling up the plug. Although melt pouring rate was not measured in this experiments, the melt pouring is assumed with free fall condition.

The flow channel section is the L-shaped conduction wall that was inclined with a certain angle. This experiment used brass and copper as wall material. Material properties of wood's metal, brass and copper can be seen on table 1. The

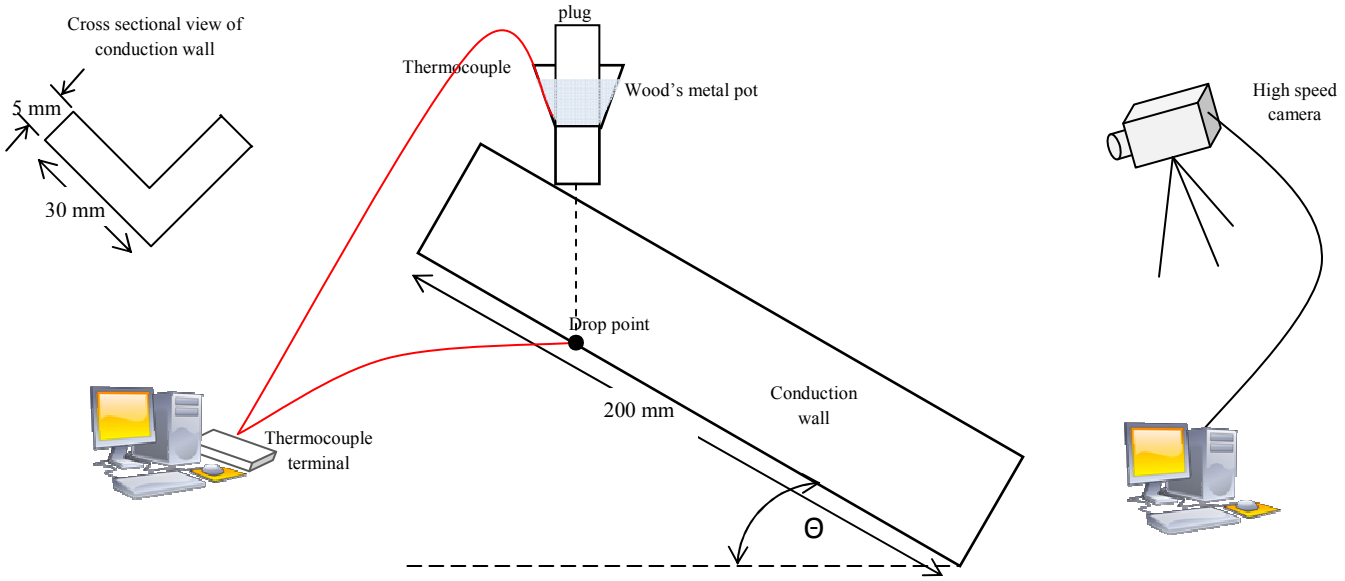

Fig. 2 Experimental Apparatus

dimension of L-shaped material is 200 x 30 x 5 mm in length, width and thick, respectively. Inclination angle of conduction wall, ϴ, is set to 15° and 30°. We set this small inclination angle to limit the penetration length, which may not exceed the conduction wall length.

Tabel 1. Material Properties

Properties	Wood's Metal		Brass (solid)	Copper (solid)
	solid	liquid		
Melting point [°C]	78.8		875	1082
Latent heart of fusion [kJ/kg]	47.3×10^3		168×10^3	205×10^3
Density [kg/m^3]	8528	8528	8470	8940
Specific heat [J/kg/K]	168.5	190	377	385
Viscosity [Pa·s]	-	2.4×10^{-3}	-	-
Conductivity [W/m/K]	9.8	12.8	117	403

In this experiment, we use wood's metal as a simulant to observe freezing behavior of molten metal. The wood's metal is chosen considering the low melting point of wood's metal and experimental simplicity. To perform the experiment, solid wood's metal is heated up until it melts and reaches high temperature (~150ºC). This is because wood's metal has high thermal conductivity and easy to be cooled done by its interaction with air and Teflon pot. In order to keep it in liquid phase at the initial stage of experiment, heating it up to a high temperature is a necessity. When heat molten wood's metal at Teflon pot has reach near-to-freeze-temperature (~85ºC), the plug is pulled, and wood's metal is release from pot and flows on the conduction wall.

During the experiments, temperatures in the wood's metal pot and at the drop point on the conduction wall are measured by thermocouples. A high speed camera is used to capture wood's metal transient behavior and its penetration length until the freezing process finishes and wood's metal is completely penetrated on the conduction wall. Several experiments were conducted with various parameters, i.e. inclination angle, wall material and wood's metal volume (2 cc and 1 cc). The experiments were performed in about 0.2 – 0.4 second until molten wood's metal completely froze and penetrated on the wall.

4. RESULT AND DISCUSSION

4. 1. Experiment Observation

The developed 3D program code was used to simulate wood's metal freezing experiment. In this simulation, particle initial distance was set to 1 mm, and the time step was 1.0×10^{-4} s. To represent inclined wall conduction, we use a 3D rotational matrix. One of the axes was rotated by the corresponding inclination angle, while the other two are by 45º and 0º. Figure 3 shows the geometrical set up of this simulation. For boundary condition of fluid dynamic calculation, fictitious wall was used as an under layer of conduction wall to calculate pressure of fluid particles reasonably. For heat conduction calculation, dirichlet boundary condition was set at fictitious wall, i.e. the fictitious wall temperature is set as air temperature, while the conduction wall temperature will slightly increase due to heat transfer process from the melt. This calculation did not involve heat convection between wood's metal and air, because the experiments were performed in a very short time. In addition, thermal conductivity and specific heat capacity of air is relatively small compared to the conduction wall.

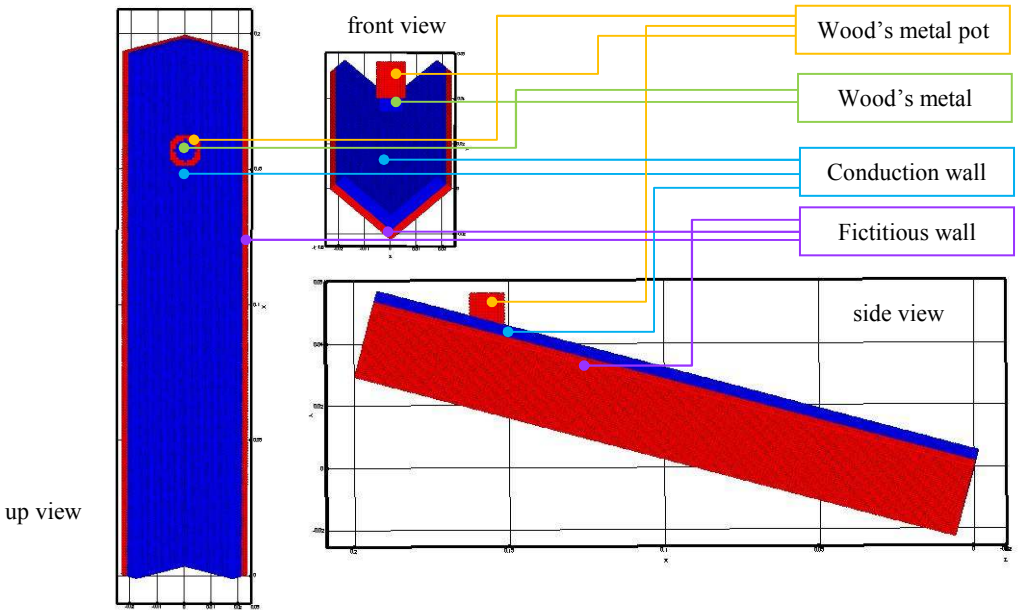

Fig. 3 Geometrical Set Up of Simulation

Therefore the heat transfer with air can be ignored.

Figure 4 shows visual comparison of the freezing process between experiment and simulation result using the experimental parameters in Table 2. The white cylinder and the grey hexagonal shaped in simulation result of Fig. 4 (left side) are intentionally added to make the visual comparisons easier.

Table 2. Experiment parameter

Wall material	Copper
Inclination angle	15º
Wood's metal volume	1 cc
Initial temperature	82.7 ºC

As can be seen in Fig. 4, the simulation and experiment results show reasonably good agreement in wood's metal shape during its freezing process. The penetration lengths of wood's metal in the experiment are reasonably simulated on the simulation. The simulation result also shows an agreement of penetration time with the experiment. After t = 0.1 second, the wood's metal is completely penetrate the wall and freeze. Thus there are no change in penetration length at t = 0.105 second.

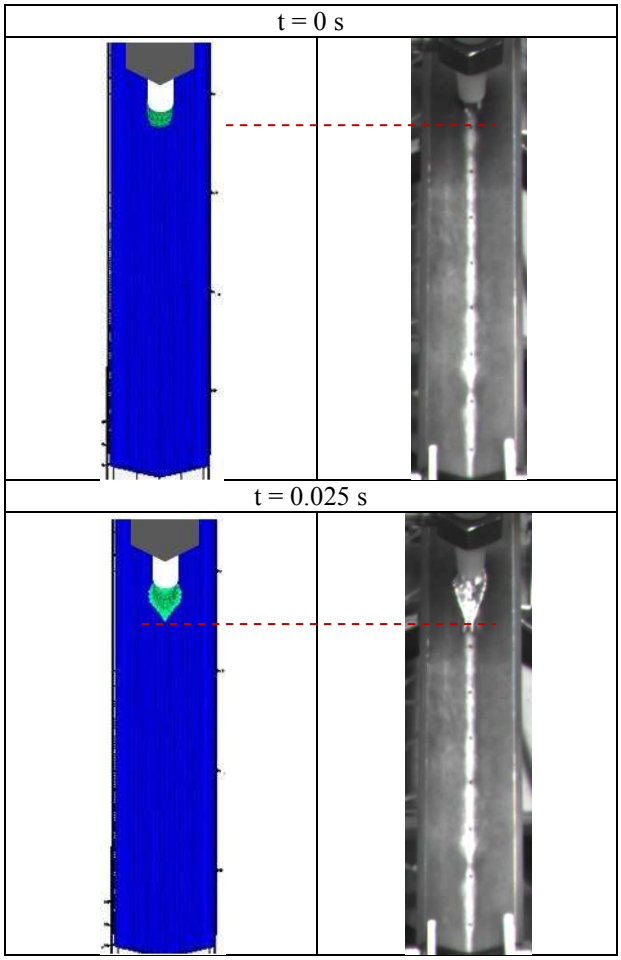

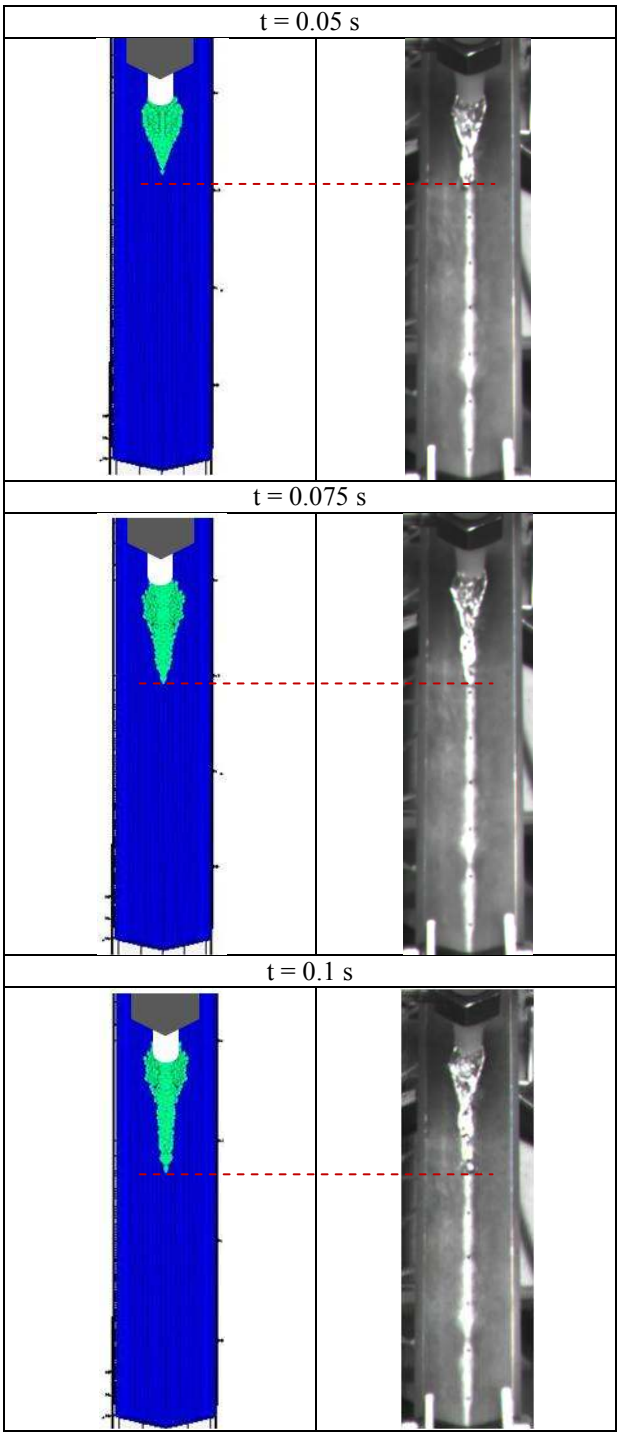

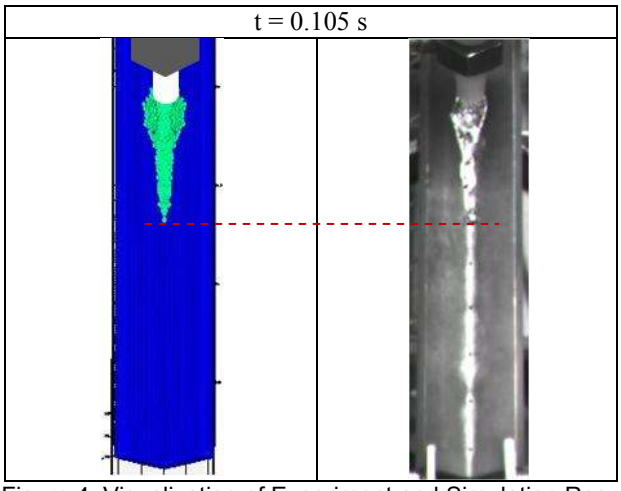

Figure 4. Visualization of Experiment and Simulation Result

The wood's metal widths on the simulation (especially at drop point) are slightly wider than the experiment due to the different size and shape of the pot's neck size. It is difficult to accurately simulate the size and shape of the pot's neck which has different upper and bottom diameter size. With this shape, after unplugging, the molten wood's metal will flow on the pot's neck and reach the conduction wall with inhomogeneous velocity. This inhomogeneous velocity makes the molten metal flows inconsecutively and results in unsymmetrical shape. In the developed code, the pot's neck is cylinder shape with 0.7 cm diameter (slightly wider than the pot's neck bottom diameter). After the simulation begins, the molten wood's metal flows steadily on this cylinder shape until it reaches the conduction wall in homogeneous velocity.

Figure 4 also shows that the frozen wood's metal shape in simulation result shows symmetrical shape between right and left side, while the experiment result is not. This is because in experiment, frozen shape is very dependent on the way to unplug. While on the simulation, the initial position of the molten wood's metal is always set at the center of the conduction wall.

4. 2. Penetration Length

Figures 5 and 6 shows the penetration length of wood's metal on copper and brass conduction wall, respectively. Here, the penetration length is the length of molten wood's metal on the conduction wall measured from drop point as its zero. The penetration length profile shows a reasonably good agreement with the experiment result.

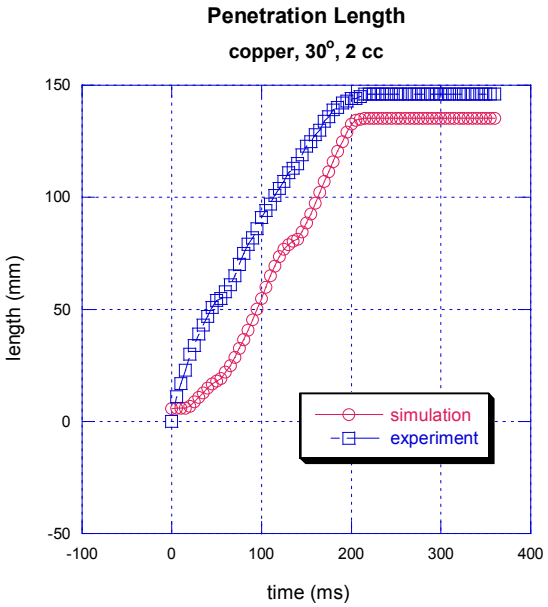

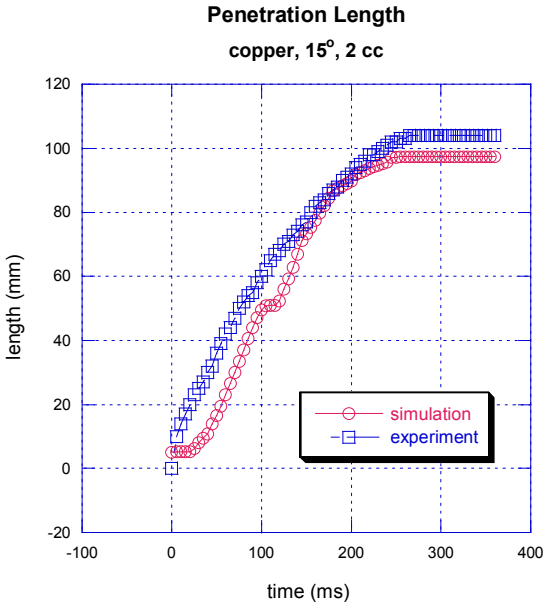

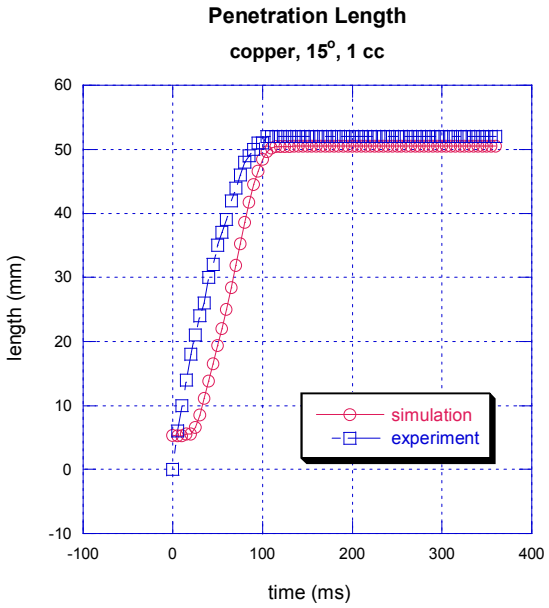

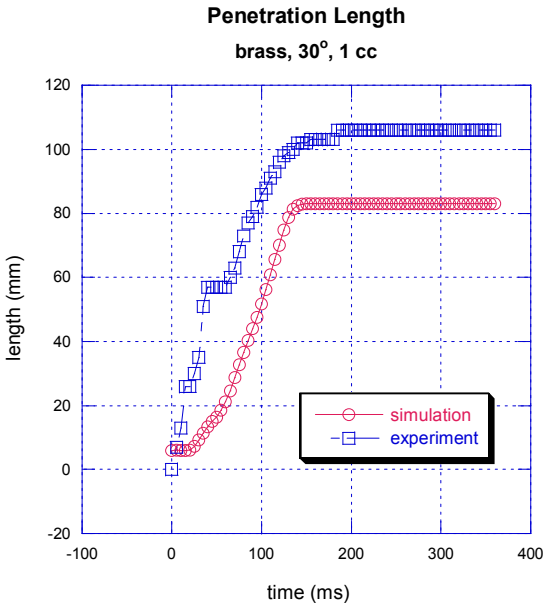

Fig. 5 Penetration Length on Copper Wall Conduction

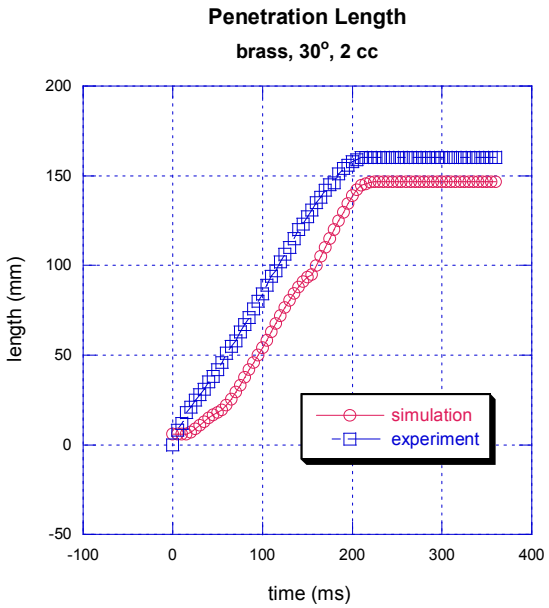

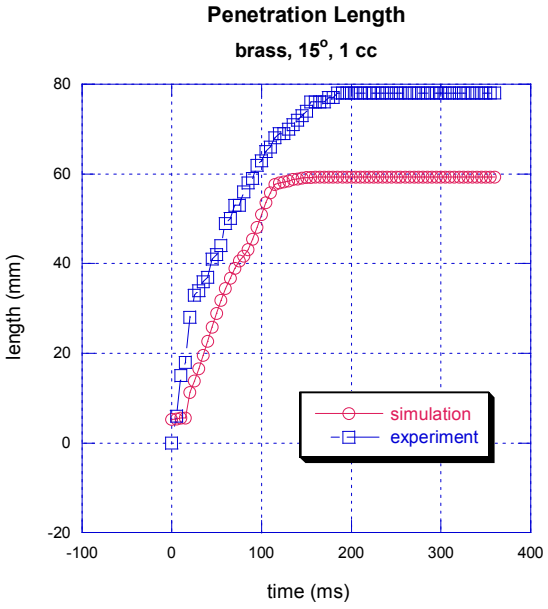

Fig. 6 Penetration Length on Brass Wall Conduction

The simulation results shows slightly shorter penetration length than the experiment result (3 mm – 2 cm shorter) due to the pouring diameter and shape differences as mentioned in previous section. In the simulation, the most bottom particles reach the wall on cylinder shape on the same time. This lead to the bigger pouring rate of wood's metal. Compared to experiments, more of wood's metals are poured in simulation in every time step. Thus, the pouring time (time to pour all of the wood's metal to the conduction wall) becomes shorter and. Due to the heat conduction, this shorter

pouring time will result in a shorter penetration length. Once the wood's metal contacts the conduction wall, heat transfer will occur. The conduction wall which has lower temperature and much larger conductivity will receive heat from the wood's metal. This transfer of heat will lead to temperature decrease of wood's metal. By Eqs (18), the temperature decrease will result in increase of viscosity force, which will suppress the particle's velocity. Therefore, the longer pouring time will result in the longer penetration length. Because once the poured molten metal froze (for example in the conduction wall that near with the pot), another "fresh-poured" molten metal is flowing on this frozen molten metal. This frozen molten metal has much slower conductivity than the conduction wall, thus the "fresh-poured" molten metal will not freeze and continue on flowing downward until it reaches the conduction wall that has no frozen molten metal yet on it. The wider pouring size also leads to the spreading of particles to the left and right side, while on the experiment this part should be flowing downward.

Figures 5 and 6 shows the same tendency of penetration length increase in every time step, except in the first 10 ms. This is because the penetration length data is obtain by measure the molten wood's metal length captured by the high speed camera. Initial penetration length always set as zero (captured by camera as no molten wood's metal yet). While in the experiment and simulation, there is no zero penetration length since initial position of the wood's metal is at the top of drop point (initial penetration length is a half of cylinder" diameter of wood's metal). It also shows that the freezing time (the time when the molten wood's metal completely penetrate on the wall) on the simulation are the same as the experiment.

4. 3. Parameters Effect on Freezing Behavior

From figures 5 and 6, we can see various parameters effect on penetration length. In conduction wall parameter, the penetration length of copper material of conduction wall is shorter than the brass material (in case of the same wood's metal volume and inclination angle). This is because copper has larger conductivity than brass, thus the heat transferred from the wood's metal to copper wall are larger than to brass wall (see Eqs (15)). This will lead to faster temperature decrease of wood's metal and shorter penetration length.

In inclination angle parameter, we can see that with the same conduction wall material and wood's metal volume, smaller inclination angle results in shorter penetration length. This is because the smaller inclination angle, the wall and particle's position becomes shorter in vertical direction. Velocity of the particle's due to height difference between particles and its neighbor in the small inclination angle is smaller than in the large inclination angle. With smaller particle's velocity, the particles will hardly move and thus the heat transfer process (especially with the conduction wall) occurs steadily. Particles with smaller velocity will freeze in shorter time than the particles with larger velocity. Therefore the penetration length becomes shorter.

5. CONCLUDING REMARKS

A 3D simulation code developed to simulate the melt freezing behavior on structure. Its model and method were verified using a series of experiments for fundamental freezing behavior of molten metal during penetration on to a metal structure. This code used finite volume particle method to solve governing equations of fluid dynamics and heat transfer calculation. The result comparison of penetration length and freezing time of wood's metal in experiment and simulation shows reasonably good agreement. Both the experiment and simulation of molten wood's metal freezing on channel flow that were conducted in various parameters are appropriate with fundamental behaviors of freezing phenomena.

NOMENCLATURE

A	Rheological parameter
C_p	Specific heat capacity [J/(kg·K)]
$\vec{f}$	Other force [N]
$\vec{g}$	Gravity [m/s^2]
h	Specific enthalpy [J/kg]
k	Thermal conductivity [W/m•K]
Δl	Initial particle distance [m]
m	Mass [kg]
n^0	Initial number density of the particles
$\vec{n}$	Unit vector
P	Pressure [Pa]
Q	Heat source [J/m^3•s]
R	Radius of control volume [m]
r_e	Cut-off radius [m]
r	Particle's position [m]
S	Surface of control volume [m^2]
ΔS	Interaction surface [m^2]
T	Temperature [K]
$T_{m/l}$	Melting temperature [K]
u	Particle velocity [m/s]
V	Volume of control volume [m^3]

Greek Letters

Θ	Inclination angle
ρ	Density [kg/m^3]
μ	Dynamic viscosity coefficient [Pa· s]
ϕ	Arbitrary scalar function
α	Liquid volume fraction

Superscript/subscript

i	Particle i
j	Particle j
l	Liquidus

ACKNOWLEDGEMENT

The present study was carried out with scholarship support from the Ministry of Education, Culture, Sports, Science and Technology of Japan. The computation was mainly carried out using the computer facilities at Research Institute for Information Technology, Kyushu University.

REFERENCES

[1] R. Wilson, Physics of Liquid Metal Fast Breeder Safety, Rev. Mod. Physics, 4 (1977).

[2] R. N. Smith and E. Meeks, Experimental Investigation of Freezing Inside a Thick-Walled Cylinder, Experimental Thermal and fluid Science, Vol. 7, No. 1, pp. 22-29 (1993).

[3] W. Liu, G. X. Wang and E. F. Matthys, Thermal Analysis and Measurements for a Molten Metal Drop Impacting on a Substrate: Cooling, Solidification and Heat Transfer Coefficient, Int. J. Heat Mass Transfer, Vol. 38, No. 8, pp.1387-1395 (1995).

[4] W. Peppler, A. Kaiser and H. Will, Freezing of a Thermite Melt Injected into an Annular Channel Experiments and Recalculations, Experimental Thermal and Fluid Sciences, Vol. 1, No. 1, pp. 335-346 (1988).

[5] H. K. Fauske, K. Koyama and S. Kubo, Assessment of FBR Core Disruptive Accident (CDA): The role and Application of General Behavior Principles (GBPs), J. Nulc. Sci. Tech., Vol. 39, No. 6, pp. 615-627 (2002).

[6] Y. Abe, T. Kizu, T. Arai, H. Nariai, K. Chitose and K. Koyama, Study on Thermal-hydraulic Behavior During Molten Material and Coolant Intraction, Nucl. Eng. Des., Vol. 230, No. 1-3, pp. 277-291 (2004).

[7] M. M. Rahman, T. Hino, K. Morita et al., ‘‘Experimental investigation of molten metal freezing on to a structure,’’ Exp. Thermal Fluid Sci., 32[1], 198 (2007).

[8] M. M. Rahman, Y. Ege, K. Morita et al., ‘‘Simulation of molten metal freezing behavior onto a structure,’’ Nucl. Eng. Des., 238[10], 2706 (2008).

[9] J.Monaghan, Smoothed particle hydrodynamics, Rep.Prog. Phys, 68 (2005)1703–1759.

[10] S.Koshizuka et al., Moving-particle semi-implicit method for fragmentation of incompressible fluid, Nucl. Sci.Eng, 123(1996) 421.

[11] K.Yabushita et al., A finite volume particle method for an incompressible fluid flow, Proceeding of Computational Engineering Conference, 10 (2005) 419-421.

[12] T. Yabe et al., An algorithm for simulating solid objects suspended in stratified flow, Computer Physics Communications, 102 (1997) 147-160.

[13] S. Zhang et al., Simulation of single bubble rising up in stagnant liquid pool with finite volume particle method, Sixth Japan-Korea Symposium on Nuclear Thermal Hydraulics and Safety, Okinawa, Japan, (2008).

[14] S.Koshizuka et al., Moving-particle semi-implicit method for fragmentation of incompressible fluid, Nucl. Sci.Eng, 123(1996) 421.

[15] A. S. Usmani, et al., Finite Element Modeling of Natural Convection-Controlled Change of Phase, International Journal for Numerical Methods in Fluids, 14 (1992) 1019-1036.

[16] V. R. Voller, An Enthalpy Method for Convection/Diffusion Phase Change, International Journal for Numerical Methods in Engineering, 24 (1987) 271-284.

[17] M. Ramacciotti et al., Viscosity models for corium melts, Nuclear Engineering and Design, 204 (2001) 377–389.

[18] M. Mooney, The viscosity of a concentrated suspension of spherical particles, J. Colloid Sci, 6 (1951) 162–170.